IOPscience iopscience.iop.org

Home Search Collections Journals About Contact us My IOPscience

Time-dependent electron tunnelling through a quantum dot with Coulomb interactions

This article has been downloaded from IOPscience. Please scroll down to see the full text article.

1997 J. Phys.: Condens. Matter 9 4875

(http://iopscience.iop.org/0953-8984/9/23/011)

View the table of contents for this issue, or go to the journal homepage for more

Download details:
IP Address: 171.66.16.207
The article was downloaded on 14/05/2010 at 08:53

Please note that terms and conditions apply.

J. Phys.: Condens. Matter **9** (1997) 4875–4886. Printed in the UK PII: S0953-8984(97)82731-2

Time-dependent electron tunnelling through a quantum dot with Coulomb interactions

Qing-feng Sun† and Tsung-han Lin†‡§‖

† Department of Physics, Mesoscopic Physics Laboratory, Peking University, Beijing 100871, People's Republic of China

‡ CCAST (World Laboratory), PO Box 8730, Beijing 100080, People's Republic of China

§ Institute of Theoretical Physics, Academia Sinica, Beijing 100080, Peoples' Republic of China

Received 19 March 1997

Abstract. Keldysh's nonequilibrium Green function is used to study the electron tunnelling through a quantum dot. Two kinds of intra-dot electron–electron (e–e) interaction are introduced: U_n for the interaction at the same energy level n with different spins, and $V_{n\sigma,m\sigma'}$ for the interaction between different levels n and m. General formulas of the time-varying current $j(t)$ and the averaged current $\langle j(t)\rangle$ are derived when the external fields are applied to the system. In the time-independent linear response regime, our calculation demonstrates that the interval of the Coulomb oscillation peaks is mainly determined by $V_{n\sigma,m\sigma'}$ which is always smaller than U_n. When the external microwave (MW) fields are applied to the system, we obtain: (1) The $j(t)$ may become negative for a certain period of time, even if the chemical potential $\mu_L(t)$ is larger than $\mu_R(t)$ all the time. (2) The calculated structure of the Coulomb oscillation peaks (in asymmetric MW fields) is in good agreement with the experimental results of Kouwenhoven *et al*. (3) For the symmetric MW field case, our theoretical results are well consistent with the experiments of Blick *et al* and Drexler *et al*.

1. Introduction

Mesoscopic physics, a new branch of condensed matter physics, has been developed and become an active field in the last decade. The quantum transport property of the mesoscopic systems is one of the most striking phenomena. Because of the possibility of designing and fabricating artificial structures, the studies on transport are no longer limited to the systems provided by nature, and have opened an extremely rich field for basic and applied researches [1, 2].

The mesoscopic transport properties studied so far are mainly related to steady-state processes. Recently, the time-dependent transport phenomena have been attracting more and more attention. The essential feature of mesoscopic physics is the phase coherence of the charge carriers. For the time-dependent processes, generally, the external time-dependent perturbation affects the phase coherence differently in different parts of the system [3, 4]. A new energy scale $\hbar\omega$ in the time-dependent problem appears. A number of new effects have been observed such as the photon–electron pump, the sideband effect, the turnstiles, the ac response in resonant-tunnelling devices, etc.

Theoretically, Tien and Gordon studied the effect of MW radiation on superconducting tunnelling devices back in the early sixties [5]. Since then, different theoretical approaches

‖ Permanent address and address for correspondence: Department of Physics, Peking University, Beijing 100871, People's Republic of China.

0953-8984/97/234875+12$19.50 © 1997 IOP Publishing Ltd

have been developed, such as the time-dependent Schrödinger equation [6, 7, 8], the transfer Hamiltonian [2, 9], the Master equation [10, 11], the Wigner function [12] and the nonequilibrium-Green-function method [3, 4, 13, 14].

Although for many mesoscopic systems the electron–electron interaction is not important and the single-electron approximation can be used very well, quite a few phenomena exist in which the electron–electron interaction plays a crucial role. The well known example is the Coulomb blockade.

In this paper we consider a quantum dot with multiple energy levels and coupled to two leads. Two kinds of intra-dot Coulomb interaction are introduced: U_n for the interaction at the same level n with different spins; $V_{n\sigma,m\sigma'}$ for the interaction between the different levels n and m. Moreover, time-dependent external fields are applied to the two leads and the dot. By using the nonequilibrium-Green-function method, the general formulas of the time-varying current $j(t)$ and the averaged current $\langle j(t)\rangle$ are derived. In the time-independent linear response regime, our calculation demonstrates that the interval between the Coulomb oscillation peaks is mainly determined by the interaction $V_{n\sigma,m\sigma'}$ which is always smaller than the interaction U_n. When external microwave (MW) fields are applied to the system, we obtain: (1) The $j(t)$ may become negative for a certain period of time, even if the chemical potential $\mu_L(t)$ is larger than $\mu_R(t)$ all the time. This new feature is quite different from the classical current–voltage character and is a manifestation of the phase coherent time-varying behaviour of the mesoscopic system. (2) For the asymmetric MW field case, the calculated structure of the Coulomb oscillation peaks is in good agreement with the experimental results of Kouwenhoven *et al* [15]. (3) For the symmetric MW field case, our theoretical studies show that some additional peaks emerge in the curves of $\langle j\rangle$ against gate voltage v_g, which are well consistent with the experiments of Blick *et al* [16] and Drexler *et al* [17]. In particular, we present a clear explanation for the peak marked with 'X' in the paper by Blick *et al* which has not been understood before.

In order to use the nonequilibrium-Green-function method for time-dependent processes, the frequencies of the external fields must be limited, and the upper limit can be up to tens of THz [3]. In this situation, one can use the adiabatic approximation, i.e. the external fields do not change the electronic distribution function directly, instead, the fields only change the single-electron energies adiabatically.

The outline of this paper is as follows. In section 2, the model is presented and the Keldysh nonequilibrium Green function is used to derive the time-dependent current formulas. In section 3, we study the time-independent case. The effects of the external MW fields are studied in section 4. A brief summary is presented in section 5.

2. Model and formulation

We assume that the system under consideration is described by the following Hamiltonian $H(t)$:

$$H(t) = H_{lead}(t) + H_{dot}(t) + H_T$$

where

$$H_{lead}(t) = \sum_{k\in L,\sigma} \varepsilon_{k\sigma}(t) a^\dagger_{k\sigma} a_{k\sigma} + \sum_{p\in R,\sigma} \varepsilon_{p\sigma}(t) b^\dagger_{p\sigma} b_{p\sigma}$$

$$H_{dot}(t) = \sum_{n\sigma} \varepsilon_{n\sigma}(t) c^\dagger_{n\sigma} c_{n\sigma} + \sum_n U_n c^\dagger_{n\uparrow} c_{n\uparrow} c^\dagger_{n\downarrow} c_{n\downarrow}$$

$$+\frac{1}{2}\sum_{n\sigma,m\sigma'(n\neq m)} V_{n\sigma,m\sigma'}c^{\dagger}_{n\sigma}c_{n\sigma}c^{\dagger}_{m\sigma'}c_{m\sigma'} \tag{1}$$

$$H_T = \sum_{k,n\sigma} L_{k\sigma,n\sigma}a^{\dagger}_{k\sigma}c_{n\sigma} + \sum_{p,n\sigma} R_{p\sigma,n\sigma}b^{\dagger}_{p\sigma}c_{n\sigma} + \text{HC}.$$

$H_{lead}(t)$ describes noninteracting electrons in the leads, $a^{\dagger}_{k\sigma}$ ($a_{k\sigma}$) and $b^{\dagger}_{p\sigma}$ ($b_{p\sigma}$) are the creation (annihination) operators of the electron in the left and the right lead, respectively. The $H_{dot}(t)$ models the quantum dot with multiple energy levels by index n and the spin σ. Two kinds of intra-dot Coulomb interaction are introduced: U_n for the e–e interaction between the electrons at the same energy level n with different spins, and $V_{n\sigma,m\sigma'}$ between the electrons with different energy levels. H_T denotes the tunnelling part which is time independent. Under the adiabatic approximation, the time-dependent external fields can be contained in the single-electron energies $\varepsilon_{\alpha\sigma}(t)$ (where $\alpha = n, k, p$ corresponds to the dot, the left lead and the right lead, respectively). However, the distribution of occupation of electrons in the leads remains unchanged [3, 4]. We separate $\varepsilon_{\alpha\sigma}(t)$ into two parts: $\varepsilon_{\alpha\sigma}(t) = \varepsilon_{\alpha\sigma} + \Delta_{\beta}(t)$, where $\beta = L, R, d$ corresponds to the left lead, the right lead and the dot, respectively; $\varepsilon_{\alpha\sigma}$ is the time-independent single-electron energies without the time-dependent external fields, and $\Delta_{\beta}(t)$ is a time-dependent part from the external fields.

Following the procedure of Wingreen *et al* [3, 4], we derive the general time-dependent current formula $j(t)$ by using the nonequilibrium-Green-function technique. The current from the left lead to the quantum dot can be calculated from the evolution of the total number operator of the electrons of the left lead, $N_L = \sum_{k\sigma} a^{\dagger}_{k\sigma}a_{k\sigma}$. Then one finds (in units of $\hbar = 1$)

$$j_L(t) = -e\langle \dot{N}_L\rangle = \mathrm{i}e\langle [N_L, H(t)]\rangle = 2e\,\mathrm{Re}\sum_{k,n\sigma} L_{k\sigma,n\sigma}G^{<}_{n\sigma,k\sigma}(t,t). \tag{2}$$

Here we define the Green function $G^{<}_{n\sigma,k\sigma}(t,t') \equiv \mathrm{i}\langle a^{\dagger}_{k\sigma}(t')c_{n\sigma}(t)\rangle$. With the help of the Dyson equation, the Green function $G^{<}_{n\sigma,k\sigma}(t,t')$ can be written as:

$$G^{<}_{n\sigma,k\sigma}(t,t') = \sum_{n'}\int \mathrm{d}t_1\, L^{*}_{k\sigma,n'\sigma}\left[G^{r}_{n\sigma,n'\sigma}(t,t_1)g^{<}_{k\sigma}(t_1,t') + G^{<}_{n\sigma,n'\sigma}(t,t_1)g^{a}_{k\sigma}(t_1,t')\right] \tag{3}$$

where $G^{r}_{n\sigma,n'\sigma}(t,t_1) \equiv -\mathrm{i}\theta(t-t_1)\langle\{c_{n\sigma}(t), c^{\dagger}_{n'\sigma}(t_1)\}\rangle$, $G^{<}_{n\sigma,n'\sigma}(t,t_1) \equiv \mathrm{i}\langle c^{\dagger}_{n'\sigma}(t_1)c_{n\sigma}(t)\rangle$, and $g^{<}_{k\sigma}$, $g^{a}_{k\sigma}$ are the exact Green functions of the electron in the left lead without coupling between the leads and the dot. Substituting the expression of $G^{<}_{n\sigma,k\sigma}(t,t)$ into (2), the sum over k, $\sum_{k\sigma}$, can be changed into an integral with the help of the density of states in the left leads, $\sum_{\sigma}\int \mathrm{d}\varepsilon\, \rho^{\sigma}_{L}(\varepsilon)$. It is useful to define:

$$\Gamma^{L}_{n\sigma,n'\sigma}(\varepsilon,t_1,t) = 2\pi\rho^{\sigma}_{L}(\varepsilon)L_{n\sigma}(\varepsilon)\,[L_{n'\sigma}(\varepsilon)]^{*}\,\mathrm{e}^{-\mathrm{i}\int_{t}^{t_1}\Delta_L(t_2)\,\mathrm{d}t_2} \tag{4}$$

where $L_{n\sigma}(\varepsilon_k) = L_{k\sigma,n\sigma}$. In terms of this generalized linewidth function $\Gamma^{L}_{n\sigma,n'\sigma}(\varepsilon,t_1,t)$, the time-dependent current $j_L(t)$ becomes:

$$j_L(t) = -2eIm\int_{-\infty}^{t}\mathrm{d}t_1\int\frac{\mathrm{d}\varepsilon}{2\pi}\sum_{n,n'\sigma}\Big\{\mathrm{e}^{-\mathrm{i}\varepsilon(t_1-t)}\,\Gamma^{L}_{n\sigma,n'\sigma}(\varepsilon,t_1,t) \times\Big[G^{<}_{n\sigma,n'\sigma}\big(t,t_1\big) + f_L(\varepsilon)G^{r}_{n\sigma,n'\sigma}\big(t,t_1\big)\Big]\Big\} \tag{5}$$

where $f_L(\varepsilon)$ is the Fermi distribution function in the left lead.

Then we have to calculate the Green functions $G^{r}_{n\sigma,n'\sigma}(t,t_1)$ and $G^{<}_{n\sigma,n'\sigma}(t,t')$. $G^{r}_{n\sigma,n'\sigma}(t,t_1)$ can be obtained from the equation of motion (EOM). Notice that $V_{n\sigma,n'\sigma'} =$

$V_{n'\sigma',n\sigma}$, then we have

$$\left[\mathrm{i}\frac{\partial}{\partial t}-\varepsilon_{n\sigma}\right]G^r_{n\sigma,n'\sigma}(t,t_1)=\delta(t-t')\delta_{n,n'}-\mathrm{i}U_n\theta(t-t')\langle\{\hat{N}_{n\bar{\sigma}}(t)c_{n\sigma}(t),c^\dagger_{n'\sigma}(t')\}\rangle$$
$$-\mathrm{i}\theta(t-t')\sum_{n_1\sigma_1(n_1\neq n)}V_{n\sigma,n_1\sigma_1}\langle\{\hat{N}_{n_1\sigma_1}(t)c_{n\sigma}(t),c^\dagger_{n'\sigma}(t')\}\rangle$$
$$+\sum_{k\sigma}L^*_{k\sigma,n\sigma}G^r_{k\sigma,n'\sigma}(t,t')+\sum_{p\sigma}R^*_{p\sigma,n\sigma}G^r_{p\sigma,n'\sigma}(t,t') \tag{6}$$

where $\hat{N}_{n\sigma}(t)\equiv c^\dagger_{n\sigma}(t)c_{n\sigma}(t)$ is the occupation number operator of the state (n,σ). The two new Green functions $G^r_{k\sigma,n'\sigma}(t,t')$ and $G^r_{p\sigma,n'\sigma}(t,t')$ are defined as $G^r_{k\sigma,n'\sigma}(t,t')\equiv -\mathrm{i}\theta(t-t')\langle a_{k\sigma}(t),c^\dagger_{n'\sigma}(t')\rangle$ and $G^r_{p\sigma,n'\sigma}(t,t')\equiv-\mathrm{i}\theta(t-t')\langle b_{p\sigma}(t),c^\dagger_{n'\sigma}(t')\rangle$. In solving (6), the new Green functions must be expressed in terms of $G^r_{n_1\sigma,n_2\sigma}(t,t')$ in order to close the equation of the Green function $G^r_{n\sigma,n'\sigma}(t,t')$. Therefore, the higher-order two-particle Green functions $\langle\{\hat{N}_{n\bar{\sigma}}(t)c_{n\sigma}(t),c^\dagger_{n'\sigma}(t')\}\rangle$ and $\langle\{\hat{N}_{n_1\sigma_1}(t)c_{n\sigma}(t),c^\dagger_{n'\sigma}(t')\}\rangle$ must be decoupled. We take the following decoupling approximation:

$$\begin{cases}\langle\{\hat{N}_{n\bar{\sigma}}(t)c_{n\sigma}(t),c^\dagger_{n'\sigma}(t')\}\rangle\approx N_{n\bar{\sigma}}(t)\langle\{c_{n\sigma}(t),c^\dagger_{n'\sigma}(t')\}\rangle\\ \langle\{\hat{N}_{n_1\sigma_1}(t)c_{n\sigma}(t),c^\dagger_{n'\sigma}(t')\}\rangle\approx N_{n_1\sigma_1}(t)\langle\{c_{n\sigma}(t),c^\dagger_{n'\sigma}(t')\}\rangle\end{cases} \tag{7}$$

where $N_{n\sigma}(t)=\langle\hat{N}_{n\sigma}(t)\rangle$ is the occupation number of the state (n,σ). Under the conditions of low temperature $k_BT\ll\Delta\varepsilon$ (here $\Delta\varepsilon$ is the energy level spacing, but degenerate state $\Delta\varepsilon=0$ is permitted) and small bias voltage, the above decoupling approximation is quite reasonable. The retarded Green functions $G^r_{k\sigma,n'\sigma}(t,t')$ and $G^r_{p\sigma,n'\sigma}(t,t')$ can be obtained by Dyson's equation:

$$\begin{aligned}G^r_{k\sigma,n'\sigma}(t,t')&=\sum_{n_2}L_{k\sigma,n_2\sigma}\int\mathrm{d}t_1\,g^r_{k\sigma}(t,t_1)G^r_{n_2\sigma,n'\sigma}(t_1,t')\\ G^r_{p\sigma,n'\sigma}(t,t')&=\sum_{n_2}R_{p\sigma,n_2\sigma}\int\mathrm{d}t_1 g^r_{p\sigma}(t,t_1)G^r_{n_2\sigma,n'\sigma}(t_1,t').\end{aligned} \tag{8}$$

Under the wide-bandwidth approximation, the linewidth $\Gamma^\alpha_{n\sigma,n'\sigma}(\varepsilon)=2\pi\rho^\sigma_\alpha(\varepsilon)\alpha_{n\sigma}(\varepsilon)[\alpha_{n'\sigma}(\varepsilon)]^*\equiv\Gamma^\alpha$ (where $\alpha=L,R$) is a constant, independent of ε, n, n', and σ. Introducing the notation $E_{n\sigma}(t)$, $E_{n\sigma}(t)\equiv\varepsilon_{n\sigma}(t)+U_nN_{n\bar{\sigma}}(t)+\sum_{n_1\sigma_1(n_1\neq n)}V_{n\sigma,n_1\sigma_1}N_{n_1\sigma_1}(t)$, then (6) reduces to

$$G^r_{n\sigma,n'\sigma}(t,t')=g^r_{n\sigma}(t,t')\delta_{nn'}-\frac{\mathrm{i}\Gamma}{2}\int_{t'}^t\mathrm{d}t_1\,g^r_{n\sigma}(t,t_1)\sum_{n_1}G^r_{n_1\sigma,n'\sigma}(t_1,t') \tag{9}$$

where $\Gamma=\Gamma^L+\Gamma^R$ and $g^r_{n\sigma}(t,t')\equiv-\mathrm{i}\theta(t-t')\exp\{-\mathrm{i}\int_{t'}^tE_{n\sigma}(t_1)\,\mathrm{d}t_1\}$. In the following we use the cumulant expansion method to calculate the retarded Green function $G^r_{n\sigma,n'\sigma}(t,t')$. Notice that usually we have either $E_{n\sigma}(t)=E_{n'\sigma}(t)$ or $E_{n\sigma}(t)-E_{n'\sigma}(t)\gg\Gamma$. Let $D_{n\sigma}$ indicate the degeneracy of the energy level $n\sigma$ (not including the spin degeneracy); we obtain

$$\begin{cases}G^r_{n\sigma,n\sigma}(t,t')=\big(1/D_{n\sigma}\big)g^r_{n\sigma}(t,t')\left\{D_{n\sigma}-1+\exp\left\{-\big(D_{n\sigma}\Gamma/2\big)(t-t')\right\}\right\}\\ G^r_{n\sigma,n'\sigma}(t,t')=\big(1/D_{n\sigma}\big)g^r_{n\sigma}(t,t')\left\{\exp\left\{-\big(D_{n\sigma}\Gamma/2\big)(t-t')\right\}-1\right\}\\ \qquad\text{while } E_{n\sigma}(t)=E_{n'\sigma}(t)\\ G^r_{n\sigma,n'\sigma}(t,t')=0\\ \qquad\text{while } E_{n\sigma}(t)\neq E_{n'\sigma}(t).\end{cases} \tag{10}$$

Defining $G^r_{n\sigma}(t,t')$ as $G^r_{n\sigma}(t,t') \equiv \sum_{n'} G^r_{n\sigma,n'\sigma}(t,t')$, we have

$$G^r_{n\sigma}(t,t') \equiv \sum_{n'} G^r_{n\sigma,n'\sigma}(t,t') = g^r_{n\sigma}(t,t') \exp\left\{-\frac{D_{n\sigma}\Gamma}{2}(t-t')\right\}. \tag{11}$$

The next step is to calculate $G^<_{n\sigma,n'\sigma}(t,t')$. By using the Keldysh equation $G^< = (1+G^r\Sigma^r)g^<(1+\Sigma^a G^a) + G^r\Sigma^< G^a$ and the self-energy functions Σ^r, Σ^a, $\Sigma^<$, and $g^<$ which can be easily derived under the wide-bandwidth approximation:

$$\begin{aligned}
\Sigma^r_{n\sigma,n'\sigma}(t_1,t_2) &= -\frac{\mathrm{i}\Gamma}{2}\delta(t_1-t_2)\\
\Sigma^a_{n\sigma,n'\sigma}(t_1,t_2) &= \frac{\mathrm{i}\Gamma}{2}\delta(t_1-t_2)\\
\Sigma^<_{n\sigma,n'\sigma}(t_1,t_2) &= \mathrm{i}\int\frac{\mathrm{d}\varepsilon}{2\pi}\left\{f_L(\varepsilon)\Gamma^L(t_1,t_2)+f_R(\varepsilon)\Gamma^R(t_1,t_2)\right\}\mathrm{e}^{-\mathrm{i}\varepsilon(t_1-t_2)}\\
g^<_{n\sigma,n'\sigma}(t,t') &= \mathrm{i}\delta_{n,n'}\langle N_{n\sigma}\rangle \exp\left\{-\mathrm{i}\int_{t'}^{t} E_{n\sigma}(t_1)\,\mathrm{d}t_1\right\}.
\end{aligned} \tag{12}$$

Using $G^a_{n\sigma}(t,t') \equiv \sum_{n'} G^a_{n'\sigma,n\sigma} = [G^r_{n\sigma}(t',t)]^*$ yields

$$\begin{aligned}
G^<_{n\sigma,n\sigma}(t,t') &= \left(1-\frac{1}{D_{n\sigma}}\right)g^<_{n\sigma}(t,t') + \int\int \mathrm{d}t_1\,\mathrm{d}t_2\, G^r_{n\sigma}(t,t_1)\Sigma^<(t_1,t_2)G^a_{n\sigma}(t_2,t')\\
G^<_{n\sigma,n'\sigma}(t,t') &= -\frac{1}{D_{n\sigma}}g^<_{n\sigma}(t,t') + \int\int \mathrm{d}t_1\,\mathrm{d}t_2\, G^r_{n\sigma}(t,t_1)\Sigma^<(t_1,t_2)G^a_{n\sigma}(t_2,t') \qquad \text{while } E_{n\sigma}(t)=E_{n'\sigma}(t)\\
G^<_{n\sigma,n'\sigma}(t,t') &= 0 \qquad \text{while } E_{n\sigma}(t)\neq E_{n'\sigma}(t).
\end{aligned} \tag{13}$$

Introducing $A^\alpha_{n\sigma}(\varepsilon,t)$ (where $\alpha = L, R$)

$$A^\alpha_{n\sigma}(\varepsilon,t) = \int_{-\infty}^{t}\mathrm{d}t_1\, G^r_{n\sigma}(t,t_1)\exp\left\{-\mathrm{i}\varepsilon(t_1-t) - \mathrm{i}\int_t^{t_1}\Delta_\alpha(t_2)\,\mathrm{d}t_2\right\} \tag{14}$$

and substituting (11), (13) into (5), we finally obtain the time-dependent current formula

$$\begin{aligned}
j_L(t) = &-e\Gamma^L\sum_{\alpha=L,R}\sum_{n\sigma}\int\frac{\mathrm{d}\varepsilon}{2\pi}f_\alpha(\varepsilon)D_{n\sigma}\Gamma^\alpha|A^\alpha_{n\sigma}(\varepsilon,t)|^2\\
&-2e\Gamma^L\sum_{n\sigma}\int\frac{\mathrm{d}\varepsilon}{2\pi}f_L(\varepsilon)\mathit{Im}A^L_{n\sigma}(\varepsilon,t).
\end{aligned} \tag{15}$$

Since $N_{n\sigma}(t) = \mathrm{Im}\, G^<_{n\sigma,n\sigma}(t,t)$, the electron occupation number at the state $(n\sigma)$ in the dot, $N_{n\sigma}(t)$, should be calculated by the following self-consistent equation

$$N_{n\sigma}(t) = \left(1-\frac{1}{D_{n\sigma}}\right)\langle N_{n\sigma}\rangle + \sum_{\alpha=L,R}\int\frac{\mathrm{d}\varepsilon}{2\pi}f_\alpha(\varepsilon)\Gamma^\alpha|A^\alpha_{n\sigma}(\varepsilon,t)|^2. \tag{16}$$

Using $\langle j(t)\rangle = \langle j_L(t)\rangle = \langle j_R(t)\rangle$, we can obtain the averaged current $\langle j(t)\rangle$ defined as

$$\begin{aligned}
\langle j(t)\rangle \equiv \lim_{\tau\to\infty}\frac{1}{2\tau}\int_{-\tau}^{\tau}\mathrm{d}t_1\, j(t_1) = 2e\frac{\Gamma^L\Gamma^R}{\Gamma}\sum_{n\sigma}\int\frac{\mathrm{d}\varepsilon}{2\pi}\Big[&f_R(\varepsilon)\,\mathrm{Im}\langle A^R_{n\sigma}(\varepsilon,t)\rangle\\
&-f_L(\varepsilon)\,\mathrm{Im}\langle A^L_{n\sigma}(\varepsilon,t)\rangle\Big].
\end{aligned} \tag{17}$$

The expressions of the time-dependent current $j_L(t)$ (15) and the averaged current $\langle j(t)\rangle$ (17) are the central results of this work. They can be applied to a variety of quantum dot structures with multiple levels, intra-dot Coulomb interaction and external time-dependent

perturbations. In the next two sections we shall apply our current formulas to two particular cases: the time-independent linear response situation and the time-dependent situation in the presence of external MW fields.

3. The time-independent case

In the time-independent case, we simply let $\Delta_\alpha(t) = 0$ ($\alpha = L, R, d$), then the $E_{n\sigma}(t)$, $N_{n\sigma}(t)$, and $j(t)$ become time independent. By Fourier transformation we can go over to the energy variable, and easily find $A^\alpha_{n\sigma}(\varepsilon, t)$ ($\alpha = L, R$)

$$A^\alpha_{n\sigma}(\varepsilon) = \frac{1}{E_{n\sigma} - \varepsilon - \mathrm{i}D_{n\sigma}\Gamma/2}. \tag{18}$$

Substituting (18) into (17), the current j is obtained as

$$j = e\Gamma^L\Gamma^R \sum_{n\sigma} D_{n\sigma} \int \frac{\mathrm{d}\varepsilon}{2\pi} \{f_L(\varepsilon) - f_R(\varepsilon)\} \frac{1}{(\varepsilon - E_{n\sigma})^2 + (D_{n\sigma}\Gamma/2)^2}. \tag{19}$$

The self-consistent equation (17) of the electron occupation number $N_{n\sigma}$ becomes

$$N_{n\sigma} = D_{n\sigma} \int \frac{\mathrm{d}\varepsilon}{2\pi} \{f_L(\varepsilon)\Gamma^L + f_R(\varepsilon)\Gamma^R\} \frac{1}{(\varepsilon - E_{n\sigma})^2 + (D_{n\sigma}\Gamma/2)^2}. \tag{20}$$

Using (19) and (20) we can evaluate the current j with arbitrary intra-dot e–e Coulomb interaction.

In the following we shall focus on the linear response regime and consider the effect of the Coulomb interactions on the period of the Coulomb oscillation, i.e. the interval between the two neighbouring peaks. We make the further simplications (as in most of the literature): (1) Let $U_n \equiv U$ and $V_{n\sigma,n'\sigma'} \equiv V$; both are independent of n, σ, n', σ'. (2) Let $\varepsilon_{k\sigma}$, $\varepsilon_{p\sigma}$ and $\varepsilon_{n\sigma}$ be independent of spin σ (not considering the magnetic fields). (3) Let the two barriers be symmetric, i.e. $\Gamma^L = \Gamma^R \equiv \Gamma$. (4) The temperature T is taken to be zero. In our numerical calculation we take the units of $e = 1$. Figure 1 shows the current j against gate voltage $v_g = -\varepsilon_1$ at small bias voltage. One notices that if $U < V$ two series of peaks with different intervals emerge (see figure 1(a)); while $U > V$ only one series of peaks appears with almost the same interval $V + \Delta\varepsilon$ (see figure 1(b)) (if we neglect the small diifference stemming from $\Delta\varepsilon$).

Although if $U = 0$ (a special case of $U < V$) but $V \neq 0$, one also has a series of equal-interval oscillation peaks, if one uses the same values of U and V to describe the turnstile effect, one will find that the height of the steps in the current–voltage curve will be $2\,ef$ (where f is the frequency of the external field) instead of $1\,ef$. This is inconsistent with the experimental result of the turnstile effect [18]. Therefore we come to the conclusion that the interval of the Coulomb oscillation peaks is mainly determined by the smaller interaction $V_{n\sigma,m\sigma'}$, not by the larger interaction, U. Here we would point out that the Coulomb interaction used in the spinless-electron quantum dot model [19] (usually denoted by U) is in fact V of this work.

Why is the interval of the Coulomb oscillation peaks more or less the same and mainly determined by the smaller interaction, V, not the larger one, U? It can be understood with the help of figure 2 which schematically describes the electronic energy levels of the quantum dot for a specific number of electrons, including the e–e interactions. Figure 2 is constructed by the following rules: (1) Electrons always occupy the lowest unoccupied states. (2) After the occupation by an electron of the state $n\sigma$ with the energy of $\varepsilon_{n\sigma}$, the state energy $\varepsilon_{n\bar{\sigma}}$ will be increased by U, and all other states will be increased by V. A Coulomb oscillation peak corresponds to the addition of an electron to the dot [20], and

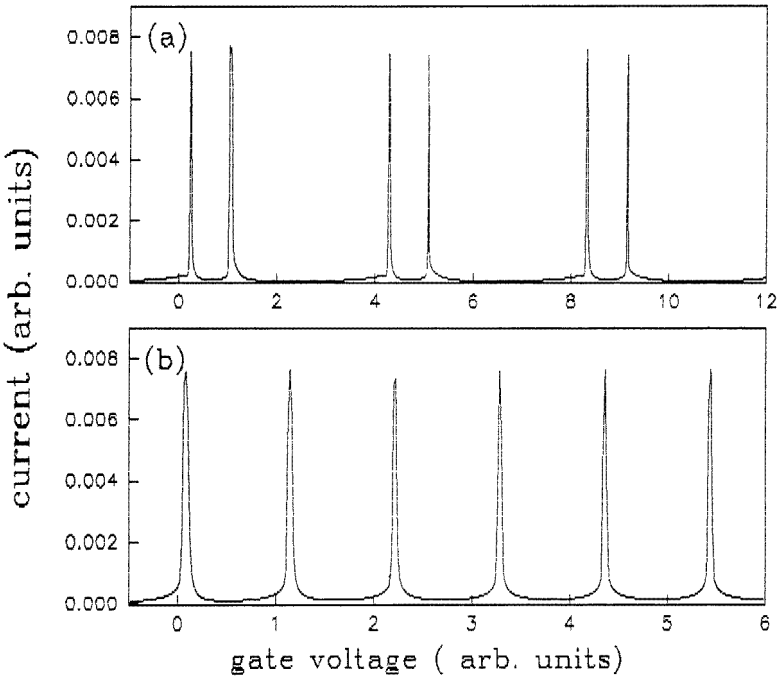

Figure 1. j against v_g for a quantum dot at small bias dc voltage $v = \mu_L - \mu_R = 0.1$ ($\mu_L = 0.1$, $\mu_R = 0$), showing the Coulomb-blockade oscillations. There are ten energy levels with $\Delta\varepsilon = 0.1$ and $\Gamma = 0.04$. (a) $U = 1$, $V = 2$. (b) $U = 3$, $V = 1$.

the interval of the peaks is the difference between the lowest unoccupied level and the highest occupied level. Figure 2(a), (b), and (c) show the electronic energy levels for the three lowest electron numbers (N) in the dot, $N = 0$, 1, and 2, respectively. Starting from the lowest state, the electrons will occupy the next higher states one by one: $(1\sigma_1)$, $(2\sigma_2)$, $(3\sigma_3)$, ... It can be easily found that the interval of the peaks is about $V + \Delta\varepsilon$. Finally the state $1\bar{\sigma}_1$ may be occupied. One can easily check that the interval is still about $V + \Delta\varepsilon$ (see figure 2(d)).

4. Time-dependent harmonic MW fields

For simplicity, we only consider the harmonic MW fields, i.e. $\Delta_\alpha(t) = \Delta_\alpha \cos \omega t$ ($\alpha = L, R, d$), and take the approximation for $E_{n\sigma}(t)$, $E_{n\sigma}(t) \approx \varepsilon_{n\sigma}(t) + U\langle N_{n\bar{\sigma}}(t)\rangle + V\sum_{m\sigma'(m\neq n)}\langle N_{m\sigma'}(t)\rangle$. Then $A^\alpha_{n\sigma}(\varepsilon, t)$ ($\alpha = L, R$) reduces to

$$A^\alpha_{n\sigma}(\varepsilon, t) = \sum_{k,k'} J_k\left(\frac{\Delta_\alpha - \Delta_d}{\omega}\right) J_{k'}\left(\frac{\Delta_\alpha - \Delta_d}{\omega}\right) \frac{\mathrm{e}^{\mathrm{i}(k-k')wt}}{\varepsilon - E_{n\sigma} + k'\omega + \mathrm{i}\frac{D_{n\sigma}\Gamma}{2}} \tag{21}$$

where the J_k are Bessel functions of the first kind. Substituting (21) into (15), we obtain the time-dependent current $j_L(t)$. Figure 3 shows $j_L(t)$ against time t at different $v_g = -\varepsilon_1$ for small bias voltage and asymmetric MW fields. From figure 3 one can find $\langle|j(t)|\rangle \gg \langle j(t)\rangle$. It is interesting to notice that the time-dependent current $j(t)$ may become negative for a certain period of time, even if the chemical potential $\mu_L(t)$ has been maintained larger than $\mu_R(t)$ all the time, i.e., $\mu_L(t) = \mu_L + \Delta_L(t) > \mu_R(t) = \mu_R + \Delta(t)$. This behaviour will not

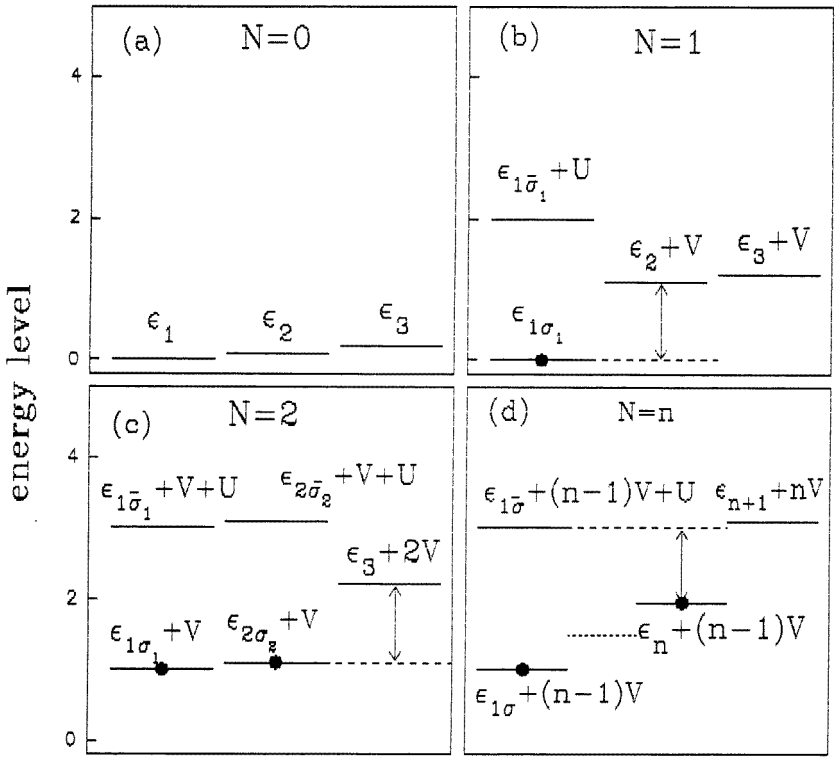

Figure 2. A schematic diagram for the electronic energy levels of the dot including the e–e interactions with $U = 2$, $V = 1$, and $\Delta\varepsilon = 0.1$. (a), (b), and (c) correspond to the three lowest numbers of electrons in the dot, $N = 0, 1, 2$, respectively. (d) shows the interval between the the new occupied state $\varepsilon_{1\bar{\sigma}_1}$ and the highest already occupied state, which is still about $V + \Delta\varepsilon$. The arrow gives the interval of two neighbouring peaks.

happen for a classical system, and is an essential feature of the mesoscopic system which comes from the phase coherence.

Substituting (21) into (17), the averaged current $\langle j(t)\rangle$ is obtained

$$\langle j(t)\rangle = e\Gamma^L\Gamma^R \sum_{k,n\sigma} D_{n\sigma} \int \frac{\mathrm{d}\varepsilon}{2\pi}\left[f_L(\varepsilon) J_k^2\left(\frac{\Delta_L - \Delta_d}{\omega}\right) - f_R(\varepsilon) J_k^2\left(\frac{\Delta_R - \Delta_d}{\omega}\right)\right] \frac{1}{(E_{n\sigma} - \varepsilon - k\omega)^2 + (D_{n\sigma}\Gamma/2)^2}. \tag{22}$$

Two special situations will be studied in the following.

4.1. Asymmetric case ($\Delta_d = \Delta_R = 0$, $\Delta_L \neq 0$)

At small dc bias voltage we obtain the characteristics of $\langle j\rangle$ against v_g (see figure 4) which has: (1) a 'shoulder' on the left side and a negative current on the right side of each Coulomb oscillation peak; (2) with the increase of Δ_L, the 'shoulder' getting higher and the negative current getting larger; (3) the location of the 'shoulder' and the negative current only dependent upon the frequency ω of the MW field. Our theoretical result mentioned above is in good agreement with the experiment by Kouwenhoven *et al* [15].

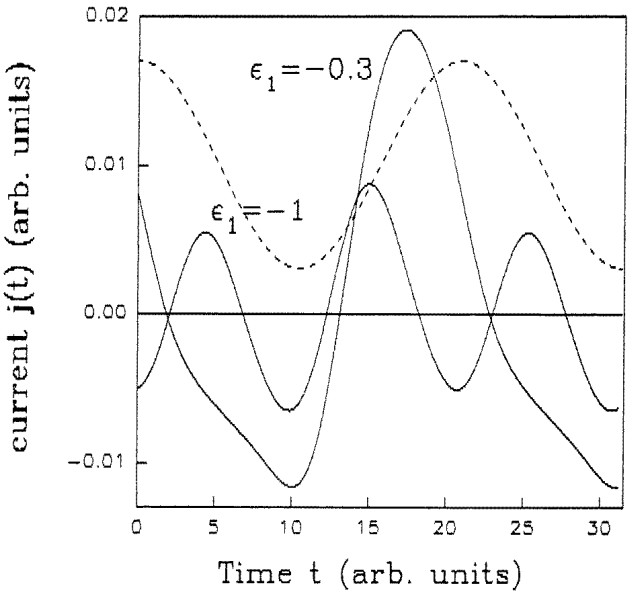

Figure 3. $j_L(t)$ against t at different v_g in the presence of harmonic MW fields with only two states $\varepsilon_{1\sigma}$, $\varepsilon_{1\bar{\sigma}}$ in the dot, and $U = 2$, $\Gamma = 0.2$, $v = 0.1$. The two solid lines correspond to $v_g = -\varepsilon_1 = 0.3, 1$, respectively. The parameters of the MW fields are: $\omega = 0.3$, $\Delta_L/\omega = 0.7$, $\Delta_R/\omega = 0.4$, $\Delta_d/\omega = 0$. The dotted line shows $v(t) = \mu_L(t) - \mu_R(t)$ against t (drawn not to scale).

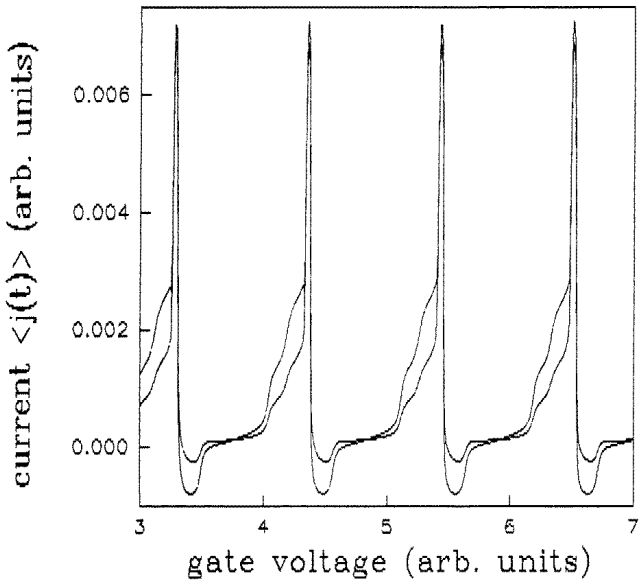

Figure 4. $\langle j \rangle$ against v_g for MW field only applied on the left lead (asymmetric case). Where $\omega = 0.3$, $\Delta_L/\omega = 0.5, 0.7$ respectively. Other parameters are the same as in figure 1(b).

4.2. Symmetric case ($\Delta_L = \Delta_R$, $\Delta_d = 0$)

Figure 5 shows the averaged current $\langle j \rangle$ against v_g in which many additional peaks emerge. When $\omega < V$, the additional peaks are located at $n\hbar\omega$ ($n = \pm 1, \pm 2, \ldots$) from the

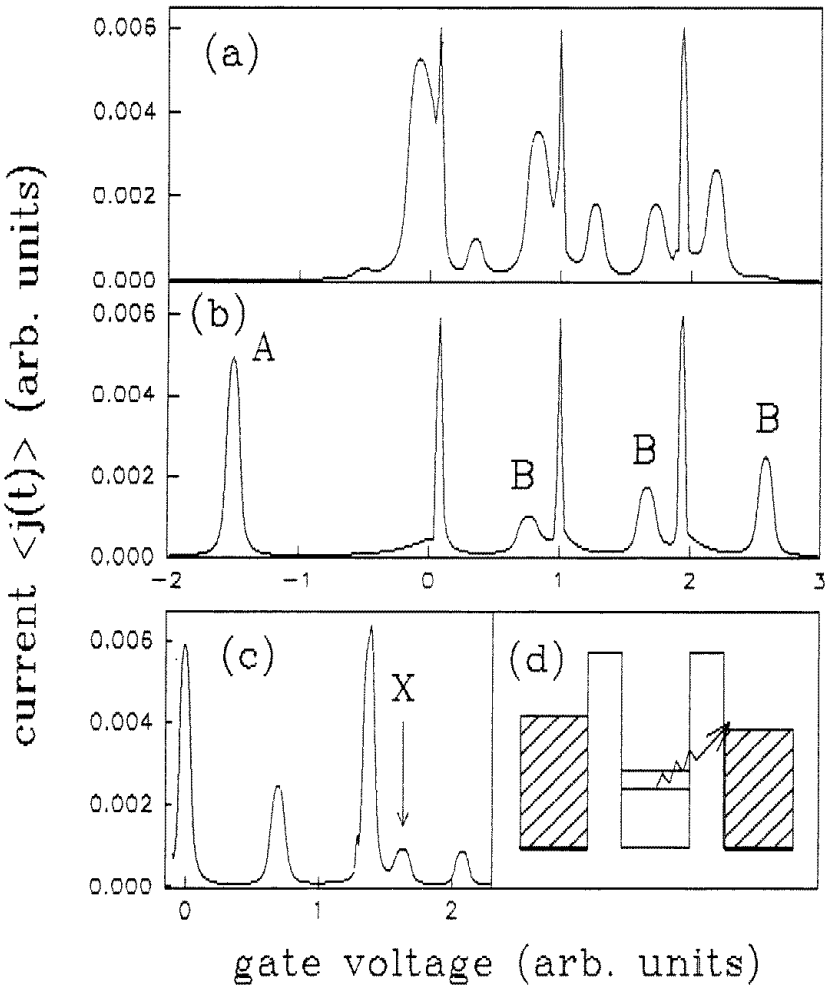

Figure 5. $\langle j \rangle$ against v_g for symmetric MW fields applied on the two leads, where $v = 0.1$, $\Gamma = 0.04$, $U = 2.2$, $V = 1$, $\Delta/\omega = 0.7$. Three degenerate levels in the dot ($D = 3$) are considered, with $\omega = 0.3$ in (a) and $\omega = 1.5$ in (b). (For descriptions of the peaks marked with A and B see text); two levels with $\Delta\varepsilon = 0.4$ and $\omega = 0.7$ in (c). (d) illustrates the location of the state in the dot corresponding to the X-peak at $v_g = 1.7$.

original Coulomb oscillation peaks, but are asymmetric to the main peak (figure 5(a)). The asymmetry comes from the difference of the number of states participating in the photon-assisted-tunnelling (PAT) processes. Our result is in good agreement with the experiment by Drexler *et al* [17].

When $\omega > V$, one can find three kinds of peak: the first is the original Coulomb oscillation peaks; the second is the peaks marked with 'A' (in figure 5(b) only one of them is shown); the third one is the peaks marked with 'B'. The A-type peak is the conventional PAT peak which is located at $n\bar{h}\omega$ from the main peak. The B-type peak is still a PAT peak, but is not located at $n\bar{h}\omega$ from the main peak. As an example let us consider the first B-type peak located at $v_g = U - \omega$. It is the PAT process originating from the unoccupied

state $(1\bar{\sigma})$ with the energy of $\varepsilon_{1\bar{\sigma}} + U$.

It is interesting to notice that even when $\omega < V$, if a certain condition is satisfied, the peaks not located at $n\hbar\omega$ from the main peak still may emerge, as well as the conventional PAT peaks. In figure 5(c) one such peak marked with 'X' is shown. It can be understood by a similar PAT process as the B-type peak mentioned above. Different from the B-type peak, the 'X' peak is the PAT process originating from the state (1σ) with the energy of $\varepsilon_{1\sigma} + V$. Figure 5(d) illustrates the electronic states in which this PAT process happens. This is well consistent with the experimental result of Blick *et al* [16] (see figure 3(b) in their paper). To our knowledge, no explanation has been given for this 'X' peak before.

5. Conclusions

In this paper we use the nonequilibrium-Green-function method to study the time-dependent tunnelling through a quantum dot with Coulomb interactions. In the absence of MW fields, we address a new explanation for Coulomb oscillation peaks. In the presence of harmonic MW fields, our theoretical results for $j(t)$ and $\langle j(t)\rangle$ display a diverse behaviour in the different cases. The Coulomb oscillation peaks reveal a fine structure for both symmetric and asymmetric external MW field cases, and they are in good agreement with the experimental results. However, in comparison to the experiment by Kouwenhoven *et al*, we could not obtain the changes from peak to peak. The reason might be the energy dependence and the electron-occupation dependence of Γ.

Acknowledgments

The authors acknowledge helpful discussions with Hong Zhou and Yuan-tai Du. We would like to thank Professor Cui-lin Wang and the Computer Centre of CCAST (World Laboratory) for helping us in our calculations. This work was supported by the National Natural Science Foundation of China and the Doctoral Programme Foundation of the Institution of Higher Education.

References

[1] Garcia-Calderon G 1993 *The Physics of Low-Dimensional Semiconductor Structures* ed P Butcher *et al* (New York: Plenum) p 267
[2] Johansson p 1990 *Phys. Rev.* B **41** 9892
[3] Wingreen N S, Jauho A-P and Meir Y 1993 *Phys. Rev.* B **48** 8487
[4] Jauho A-P, Wingreen N S and Meir Y 1994 *Phys. Rev.* B **50** 5528
[5] Tien P K and Gordon J P 1963 *Phys. Rev.* **129** 647
[6] Stone A D and Azbel M Ya 1985 *Phys. Rev.* B **31** 1707
[7] Sokolovski D 1988 *Phys. Rev.* B **37** 4201
[8] Liu H C 1991 *Phys. Rev.* B **43** 12 538
[9] Johansson P and Wendin G 1992 *Phys. Rev.* B **46** 1451
[10] Nazarov Y V 1993 *Physica* B **189** 57
[11] Bruder C and Schoeller H 1994 *Phys. Rev. Lett.* **72** 1076
[12] Frensley W R 1987 *Phys. Rev.* B **36** 1570
[13] Chen L Y and Ting C S 1991 *Phys. Rev.* B **43** 2097
[14] Runge E and Ehrenreich H 1992 *Phys. Rev.* B **45** 9145
[15] Kouwenhoven L P, Jauhar S, Orenstein J, McEuen P L, Nagamune Y, Motohisa J and Sakaki H 1994 *Phys. Rev. Lett.* **73** 3443
[16] Blick R H, Haug R J, van der Weide D W, von Klitzing K and Eberl K 1995 *Appl. Phys. Lett.* **67** 3924
[17] Drexler H, Scott J S, Allen S J, Campman K L and Gossard A C 1995 *Appl. Phys. Lett.* **67** 2816

[18] Kouwenhoven L P, Johnson A T, var der Vaart N C and Harmans C J P M 1991 *Phys. Rev. Lett.* **67** 1626
[19] Beenakker C W J 1991 *Phys. Rev.* B **44** 1646
[20] Meirav U, Kastner M A and Wind S J 1990 *Phys. Rev. Lett.* **65** 771